Material-Independent Mechanochemical Effect in the Deformation of Highly-Strain-Hardening Metals

Anirudh Udupa, Koushik Viswanathan, Mojib Saei, James B. Mann, and Srinivasan Chandrasekar

Phys. Rev. Applied **10**, 014009 — Published 13 July 2018

DOI: 10.1103/PhysRevApplied.10.014009

Glues make gummy metals easy to cut

Anirudh Udupa,[1] Koushik Viswanathan,[1] Mojib Saei,[1]
James B. Mann,[2] and Srinivasan Chandrasekar[1]

[1] *Center for Materials Processing and Tribology, Purdue University, West Lafayette, IN*

[2] *Department of Mechanical Engineering, University of West Florida, Pensacola, FL*

Abstract

Soft and highly strain hardening metals like iron, aluminum and tantalum, often called gummy, are notoriously difficult to cut. This is due to their tendency to exhibit redundant, unsteady plastic flow with large-amplitude folding, and which results also in macro-scale defects on the cut surface and large energy dissipation. In this work, we demonstrate that this difficulty can be overcome by merely coating the initial metal surface with common adhesive chemical media like glues and inks. Using high-speed *in situ* imaging, we show that the media act by coupling unsteady surface plastic flow modes with interface energetics - a mechanochemical action - thereby effecting a ductile-to-brittle transition, locally. Consequently, the unsteady plastic flow with folding transitions to a periodic segmentation-type flow in the presence of the surface media, with near absence of defects on the cut surface and significantly lower energy dissipation (reduction of up to 80%). This mechanochemical effect is controllable and not material specific, with the chemical media demonstrating comparable efficacy across different metal systems. This makes it quite distinct from other well-known mechanochemical effects, such as liquid metal embrittlement and stress-corrosion cracking, that are both highly material-specific and catastrophic. An analytical model incorporating local flow dynamics, stability of dislocation emission and surface media energetics is found to correctly predict the onset of the plastic flow transition. The benign nature and simplicity of the media suggests wide-ranging opportunities for improving performance of cutting and deformation processes for metals and alloys in practical settings.

I. INTRODUCTION

It is well known that soft metals, as well as metals with large strain hardening capacity, such as pure aluminum, iron, copper and tantalum are notoriously difficult to cut. This difficulty is manifest as very large forces, thick chips and a profusion of defects on the surface [1, 2]; hence, such soft metals are often called "gummy" [3]. It was shown recently that this difficulty is due to an unsteady mode of large-strain plastic deformation—sinuous flow, characterized by plastic buckling and large amplitude material folding—that prevails during cutting [2, 4–6]. If this sinuous flow mode can be disrupted and replaced by a more favorable deformation mode, with smaller forces and deformation strain, then cutting of these metals could be carried out efficiently.

A possible general route for modulating plastic flow in cutting/ processing is via utilization of mechanochemical effects—changes in mechanical response of a material in presence of a chemical medium. Mechanochemical effects have been known in some form or the other for a long time, the earliest reports perhaps dating back nearly 2000 years to the use of Hg by Roman gold miners [7]. The mechanochemical route has been exploited in processing of ceramics and other non-metals; examples include chemomechanical planarization [8, 9] and comminution [10, 11]. In metals, mechanochemical effects are regarded as being highly material specific and almost synonymous with catastrophic failure, e.g., stress corrosion cracking, liquid metal embrittlement [12–16]. A few chemical media like CCl_4 [17–20] have shown promise in favorably influencing metal cutting processes, speculated to occur via changes in the metal's ductility [21–23]. However, there are concerns about variability in reports of these effects [24–26]. Additionally, these media have critical health and environmental issues (e.g., CCl_4 is a well-known carcinogen) that far overshadow any potential utility.

Given the uncertainty in using controllable mechanochemical effects in metals, we recently revisited the role of surface-active (SA) chemical media in influencing large-strain plastic flow in metals. Surface-active is a term conventionally used to describe those media that form a strong adsorbed layer on metal surfaces and influence surface energies [24] [27]. We found that when a common metal-marking ink was coated, prior to cutting, onto the surface of commercially pure copper (which deforms by sinuous flow in the annealed condition), the cutting forces were lowered significantly [2]. This preliminary observation pointed to the more wide-ranging possibility of certain adsorptive media influencing the plastic flow process

in cutting of metals, in hitherto, unknown ways. The present work is thus an outgrowth of these preliminary observations.

In this study, we demonstrate profoundly beneficial mechanochemical effects in large strain deformation of metals using very common media such as commercial glue sticks and marking inks. The effects are shown to arise from a strong coupling between these media and the underlying plastic flow mode. The effects are widespread, controllable, materially agnostic and with scope for practical application. The demonstration is an outcome of a multiscale re-examination of mechanochemical phenomena in deformation of metals, using high-resolution *in situ* and *ex situ* observations.

The manuscript is organized as follows. The experimental setup is described in Sec. II. The primary observations of the mechanochemical effect are presented in Secs. III A—III D and an analytical model explaining the physics behind the effect is described in Sec. III E. The implications of our study are discussed in Sec. IV and concluding remarks are presented in Sec. V.

II. EXPERIMENTAL PROCEDURES

Preliminary cutting experiments with commercially pure copper have shown that application of some common chemical media to the metal surface prior to the cutting caused reductions in the cutting force and energy [2]. These effects appear to depend also on the initial strain-hardening state of the copper, with the media effect being significant in annealed copper. Motivated by these observations, the experimental program was structured to study, both, the effects of various chemical media, characterized by different adhesive coupling strengths to metal surfaces, on the plastic flow and cutting; and to examine how these effects are influenced, if at all, by the initial hardening state (e.g., annealed, pre-hardened) of the metal. This program structure thus enabled exploration of hypotheses pertaining to how media effects occur and whether these are coupled to specific flow phenomena.

The model 2-D cutting system consists of a ductile, highly strain-hardening metal workpiece cut by a hard wedge (tool) at constant velocity V_0. The tool is fixed normal to V_0, and has a constant penetration depth h_0, see **Fig. 1**. As a result, a part of the workpiece material is removed in the form of a chip (strip) of thickness h_C by plastic deformation (strains > 2). This system is well-established also as a means for imposing varying extents (controlled) of

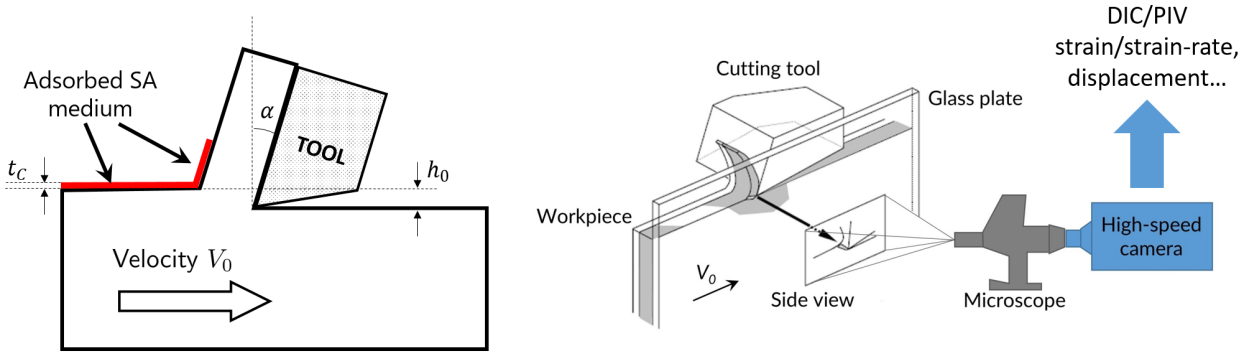

FIG. 1: Schematic of cutting configuration used in the experiments. The SA medium is applied to the workpiece free surface remote from the tool-chip interface. The deformation zone is observed *in situ* to obtain high-resolution quantitative flow field information.

large-strain, shear deformation [2]. The flow of metal in the deformation/cutting zone is observed *in situ* and captured using a high-speed camera, with images post-processed using digital image correlation (DIC) techniques to obtain quantitative flow field information (e.g., displacement/strain history, material rotation, flow lines) [28].

Three different workpiece materials, well-known for their strain-hardening capacity, were used in the cutting experiments, commercially pure Cu (99.99% OFHC Cu 101), commercially pure Al (99% Al 1100) and commercially pure Fe (99.85% ARMCO). The copper and iron samples were machined to a dimension of 75 mm × 25 mm × 6mm before annealing in an inert atmosphere (Argon). The copper was annealed at 750° C for 4 h and oven cooled, while the iron was annealed at 950° C for 4 h and oven cooled. Annealing in the inert atmosphere minimizes formation of an oxide layer on the metal surface. The hardness of annealed Cu was 68 HV and annealed Fe was 90 HV. The aluminum samples were directly procured as sheets in the annealed (O) and the half-hard (H14) state. The latter enabled study of flow-media coupling effects arising from pre-hardening of the metal before cutting. The dimensions of the aluminum workpieces were 100 mm × 25 mm × 1.5 mm. Hardness of annealed Al was 23 HV and of half-hard (H14) Al was 30 HV.

A range of chemical media were used to coat the workpiece surface prior to cutting, with the coated surface remote from the tool-chip contact **Fig. 1 left**. The selection of these media, to test various hypotheses underlying mechanochemical effects and flow, was based on considerations such as strength of their adhesive bonding via physical adsorption to the metal surface, and chemical specificity of the bonding to the metal surface. Based on this

interaction strength, the media are broadly classified into three groups.

- **Group I** consists of media that show strong physical adsorption to the three metals. The following media belong to this group. Glue 1 (Scotch restickable glue stick), Glue 2 (Scotch super glue gel), Glue 3 (Gorilla super glue), Ink 1 (Sharpie permanent marker), Ink 2 (Dykem), Ink 3 (Paper Mate Liquid Paper correction fluid).

- **Group II** consists of media that show chemical affinity (specificity) for Al only, as established by their ability to corrode oxide-free Al surfaces. The following media belong to this group. Isopropyl alcohol (Fisher Chemical), Ethanol (Decon Labs) and 1-Butanol (Fisher Chemical).

- **Group III** consists of media that are not known for any significant adsorptive or other similar interactions with any of the metals. The following media belong to this group. Distilled water, Toluene (Consolidated Chemical) and Acetone (Fisher Chemical).

Additionally, some other media, which could not be clearly classified into one of the aforementioned groups, are also studied. These include soap (Proctor and Gamble), paraffin wax (Gulf Wax), adhesive tape (Scotch transparent tape) and diacetone alcohol (Lab Alley).

The cutting was carried out using a tungsten carbide tool, carefully ground so that the cutting edge had a radius of less than 5 μm. The width of the rake face of the tool was 2.3 mm, which also corresponds to the chip width into the plane in **Fig. 1**. The initial cutting depth h_0 was fixed at 50 μm, while the cutting speed V_0 was fixed at either 2 mm/s or 15 mm/s, with no effect on the results. The low V_0 minimizes any temperature effects on the deformation. In order to ensure plane–strain deformation, side flow of the workpiece material was prevented using a quarter-inch glass plate as a lateral constraint. The media was applied to the top-surface of workpiece as shown in **Fig. 1**. The region of interest, illuminated by halogen white light (150 W), was imaged using a high-resolution CMOS camera (pco-dimax), coupled to an optical microscope (Nikon Optihphot), with a resolution of 1.4 μm per pixel and a frame rate of 200 frames per second. A piezoelectric dynamometer (Kistler 9254) was used to measure the cutting forces, with the data sampled at 900 Hz. The specific energy for cutting could be obtained from the measured force and cutting speed. The topographical characteristics of the residual cut surface were evaluated using a large-area 3D optical profilometer (Zygo NewView 8300).

The cutting was carried out both with and without a lubricant applied to the cutting zone. The lubricant when used was Mobil 1-5w30. The primary observations were unchanged in the presence of the lubricant precluding any potentially obscuring effects due to lubrication.

III. RESULTS

The high-speed imaging has enabled quantification of the flow during deformation, both with and without SA media application. We present the primary experimental results below, followed by an analytical model that captures the essential physics underlying the mechanochemical effect with SA media.

A. Sinuous flow, SA media and plastic flow transition

Sinuous plastic flow, an unsteady flow mode characterized by repeated material folding and large local strains, is the norm when cutting soft and highly strain hardening metals [2, 6]. The highly redundant deformation, due to folding, results in large cutting forces, energy dissipation and a very thick chip [4, 6]. This type of flow is nucleated by a plastic buckling instability on the material free surface [5], see **Fig. 2 top row** which shows three frames from a high-speed *in situ* image sequence. A bump, with extremities P_1, P_2 termed pinning points, results from plastic buckling on the free surface; P_1, P_2 are almost always coincident with grain boundaries and/or other local heterogeneities [5, 29]. As deformation continues, the bump grows in size, and is rotated, eventually evolving into a large amplitude fold. The process repeats with subsequent buckling events leading to adjacent folds collapsing onto each other to form the chip, as reflected by the wavy streaklines in the images.

In the presence of SA media, applied remote from the tool-workpiece interface, a distinct deviation from sinuous flow was observed—a mechanochemical effect. Three frames from a high-speed sequence showing the resulting deformation for annealed Cu with an SA medium (glue 1) are presented in **Fig. 2 bottom row**. The plastic buckling instability, with bump formation, again occurs ahead of the tool, see pinning points Q_1, Q_2 in frame 1. However, during the initial stages of the bump developing into a fold, a crack now nucleates on the free surface at the pinning point Q_1 and propagates towards the tool tip (red arrow, frame 2). This crack propagates to varying degrees, depending on the cutting conditions

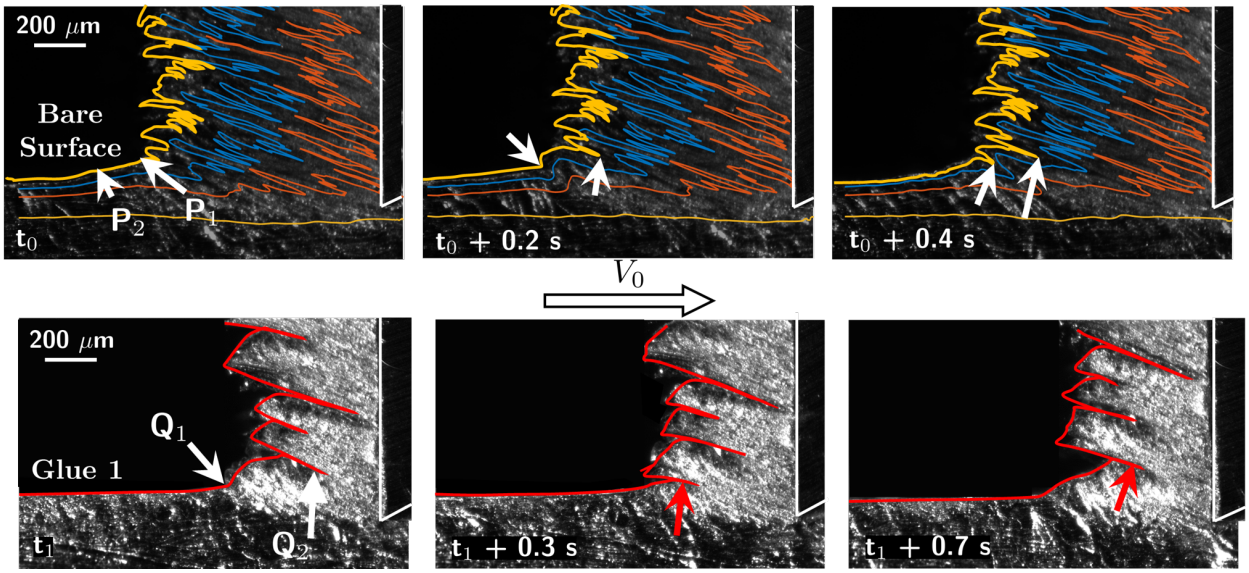

FIG. 2: High-speed *in situ* images of the deformation zone in cutting of annealed Cu. (Top row) Three frames from a sequence showing sinuous flow, absent any SA medium. This flow is characterized by large amplitude material folding, as revealed by the wavy streaklines in the workpiece. Each folding event is initiated by a buckling instability leading to formation of a surface bump bound by pinning points P_1 and P_2 (arrows, frame 1). The bump grows in size and evolves into a fold (frames 2,3) and the process repeats. (Bottom row) When an SA medium (glue 1) is applied to the Cu surface remote from the tool-chip contact, buckling still occurs, see bump bounded by pinning points Q_1 and Q_2 (frame 1). However, a fracture instability now sets in before the bump evolves into a fold, and a crack grows from the pinning point Q_1 (red arrow, frame 2). The crack is arrested close to the tool tip (frame 3); the chip is much thinner, consisting of a series of segments with each segment resulting from a crack. This type of flow is called segmented-type flow.

(α, V_0, h_0), before it is arrested (frame 3). Subsequently, another plastic buckling event is initiated and the process repeats. The development of sinuous flow with folding is thus disrupted by a 'segmented' type of flow, caused by recurring fracture in the presence of the SA medium. This transition in flow, observed with several other SA media, characterizes the mechanochemical effect. **Movie S1** explicitly demonstrates the transition in annealed Cu with SA medium (glue 1) coated along the latter half of its length.

The transition in plastic flow, from sinuous to segmentation-type when the SA media is applied, is manifested in the resulting chip. Not only is the chip now much thinner than

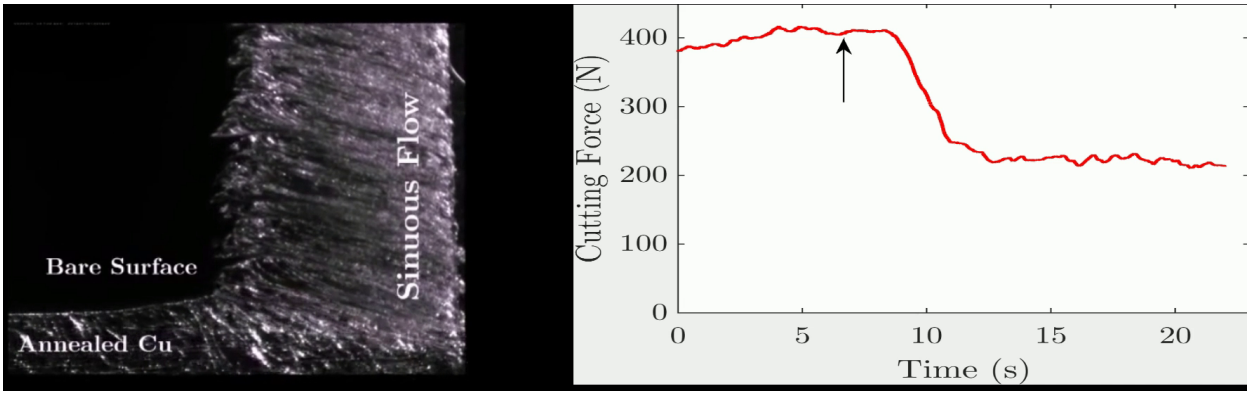

Movie S1: Transition from sinuous to segmentation-type ow due to SA media application.Annealed Cu is cut initially with an uncoated surface, resulting in sinuous ow, thick chip and a large cutting force. The latter half of the workpiece free surface (remote from tool-chip interface) is coated with Glue 1, resulting in a transition to segmentation-type ow, thin chip and a much reduced cutting force. Simultaneous variation in the force is shown on the right.

before (*cf.* **Fig. 2 top, bottom rows**) but the morphology on its free surface is also much altered, see **Fig. 3**. The characteristic mushroom-type structure (**Fig. 3a**) with sinuous flow, absent any media, is due to adjacent folds that have collapsed onto each other (yellow arrows). With the SA medium present, the chip instead has a sequence of periodically spaced 'segments' (**Fig. 3b**) with fractured surfaces (red arrows) dominating over regions with minor folding events (yellow arrows). Crucially, crack initiation sites coincide with the pinning points that bound the initial bump (Q_1, Q_2 in **Fig. 2**). Locally, these regions are shaped like notches and result in a sharp stress concentration. It is interesting that in cases where sinuous flow is absent, thereby precluding any such stress concentrators, the SA media have no influence on the process at all. This is illustrated by applying the same medium to the metal in an initially fully hardened state (pre-strain ~ 2.5). Here, it is known that the tendency for plastic buckling is much reduced [2, 5] and that the resulting flow is laminar or smooth—a fact that remains unchanged by the medium application.

B. Effect of Group I-III media on forces and energy dissipation

Perhaps the most drastic consequence of the mechanochemical effect is a consistent reduction in cutting force accompanying the change in flow/chip morphology. We tested the three

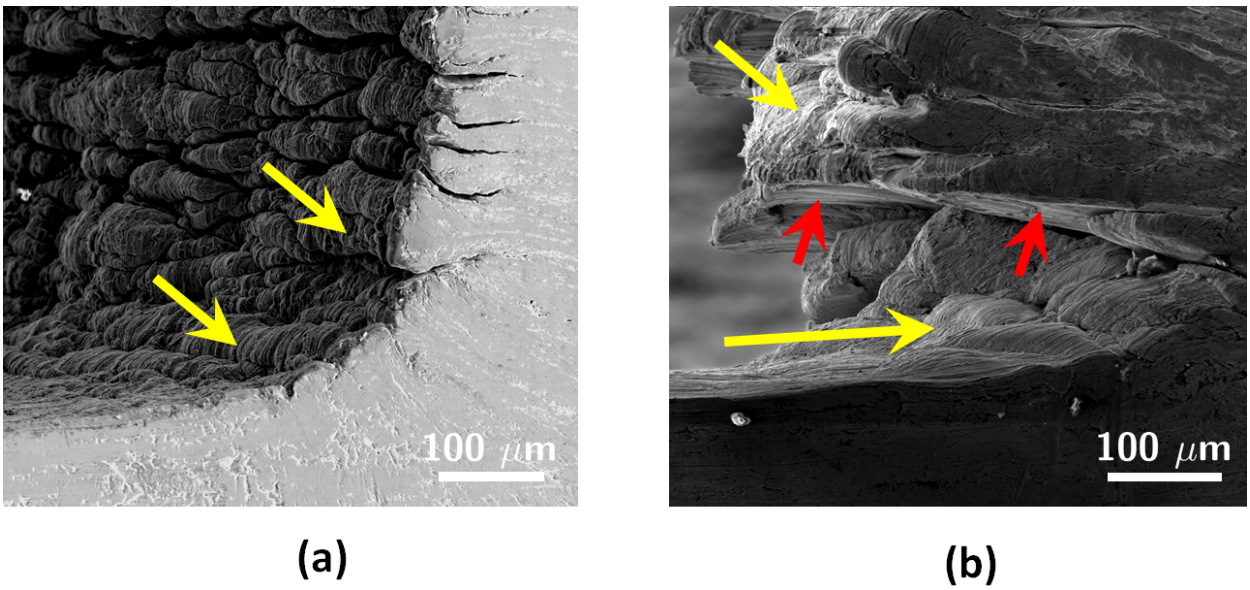

FIG. 3: Scanning electron microscopy images of chip morphology in Cu. (a) Characteristic mushroom-type structures on the chip free surface, a signature of sinuous flow, arise due to individual folds (yellow arrows) collapsing onto each other. (b) In the presence of an SA medium (glue 1), the flow transitions from sinuous to segmentation-type, characterized by minor folding events in each segment (yellow arrows) and separated by periodic fracture surfaces (red arrows). The morphologies span the entire width of the chips.

metal systems with 16 different common media, and varying tool rake angle $\alpha = 0°, 45°$ and initial workpiece condition—annealed and half-hard (H14) (see the **Experimental Procedures** section for details). In each case, the SA medium was applied on the metal's free surface, remote from the tool-chip contact interface (see **Fig. 1**). **Figure. 4** is a scatter plot of the absolute magnitude of the corresponding cutting forces (parallel to the velocity V_0 direction) when cutting bare uncoated metal (F_B) and the coated samples (F_C). Data is shown for Al and Cu, and with $\alpha = 0°$. The different metal-media combinations appear to be enveloped between the lines $F_C = F_B$ (no mechanochemical effects) and $F_C = 0.2F_B$ (largest reduction, $\sim 80\%$).

Based on the data in this figure, the SA media may be classified into three groups. Group I media showed consistent mechanochemical effects and force reductions independent of the metal to which they were applied, see **Fig. 4**. Examples in this group include commercial glues, glue 1 (Scotch glue), glue 2 (Super glue), and metal marking inks, ink 1 (Sharpie), and ink 2 (Dykem). The corresponding force reduction is $\sim 50\%$ ($F_C = 0.5F_B$), corrsponding

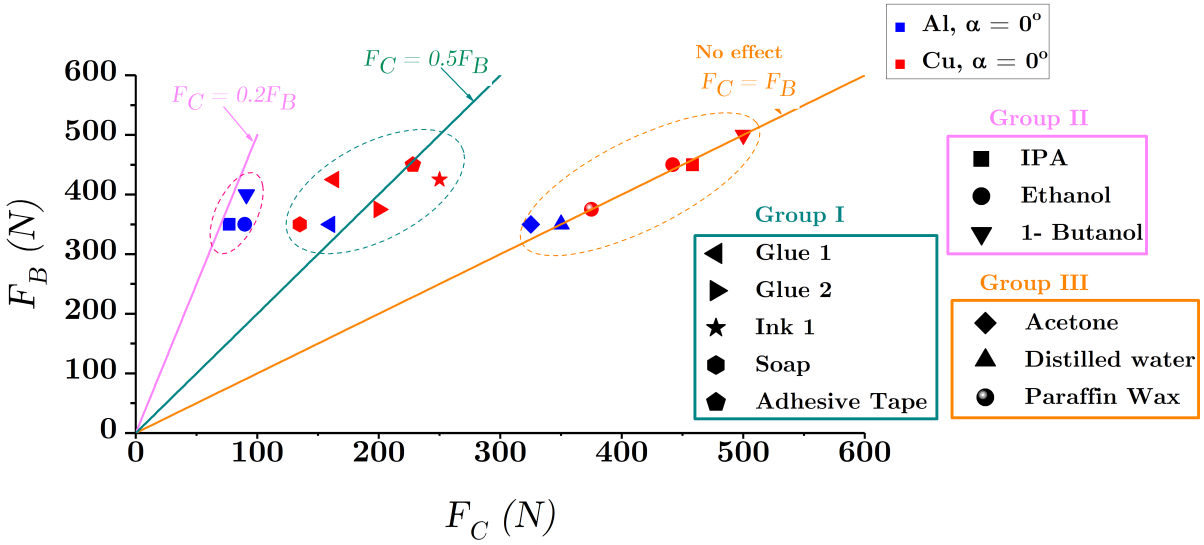

FIG. 4: Scatter plot showing cutting force values with (F_C) and without (F_B) media on various metals. The workpiece metal are indicated on the plot using different colors, whereas media are indicated using different symbols as specified in the legend. Group I media fall around the $F_C = 0.5F_B$ line, Group II on the $F_B = 0.2F_C$ line and Group III around the $F_B = F_C$ line (negligible mechanochemical effect). Al and Cu a refer to metals in annealed state.

to the points clustered around the $F_C = 0.5F_B$ line in the figure. The force reduction in each case was accompanied by a corresponding transition from sinuous to segmented-type flow (see **Movie S1**). All of the media in this category are distinguished by their ability to adhere well to metal surfaces [30].

Group II media showed pronounced effects only with some metals, and Group III media showed no effects at all ($F_c = F_B$ in **Fig. 4**). For instance, alcohols in Group II—isopropyl alcohol (IPA), butyl alcohol, ethanol—showed the largest force reductions (nearly 80%, $F_C = 0.2F_B$) with Al, yet had no effect with Cu. This is noteworthy since isopropyl alcohol, in particular, is the only common ingredient of media in Group I (e.g., inks 1 and 2) yet shows no effect with Cu and Fe (unlike inks 1 and 2 themselves). Again, this is reflective of the strength/weakness of local adhesive bonds that form at the media-metal interface: the alcohols are known to form strong bonds with Al to such an extent that they may even corrode it to form the corresponding alkoxide [31, 32]. Likewise, DI water and Toluene (Group III, little to no adhesion) showed no effects at all with any of the metals. Note that

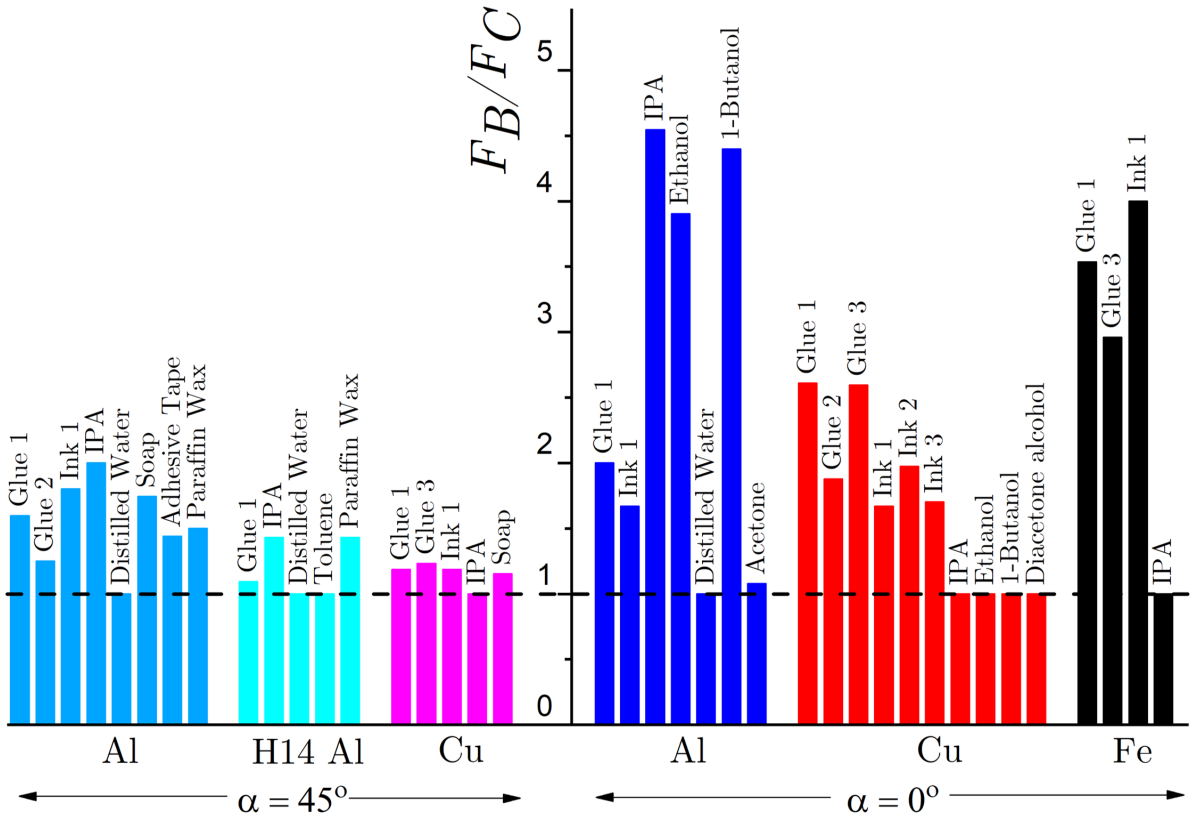

FIG. 5: Ratio of cutting force for uncoated (F_B) to SA-medium coated (F_C) workpiece samples for various SA media-metal combinations and cutting conditions. Mechanochemical effects result in force reductions of as much as 80% (Al-IPA, $\alpha = 0°$). Al, Cu and Fe refer to metals in annealed state, while H14 is a half-hard condition for Al.

the points clustered around $F_C = F_B$ consist of Group II (with Cu) and Group III (both Al and Cu) media.

A more expansive set of results with all three metals (Cu, Al, Fe) and $\alpha = 0°, 45°$ is shown in **Figure 5**. In addition to confirming the general trends discussed in 4, the bar chart also shows larger force reductions when $\alpha = 0°$ ($F_C \sim 0.5F_B$) compared to $\alpha = 45°$ ($F_C \sim 0.8F_B$). This may be directly attributed to the increased propensity for sinuous flow at $\alpha = 0°$, i.e., larger fold amplitude and thicker chip. This is also confirmed by comparing the forces for the annealed vs. half hard initial state (see Al H14, **Fig. 5**), since the latter is well known to exhibit laminar, instead of sinuous, flow [2, 5]. Since both the total energy dissipated and specific energy (energy per unit volume) of deformation are directly proportional to the cutting force, the force reductions indicate a reduction in the

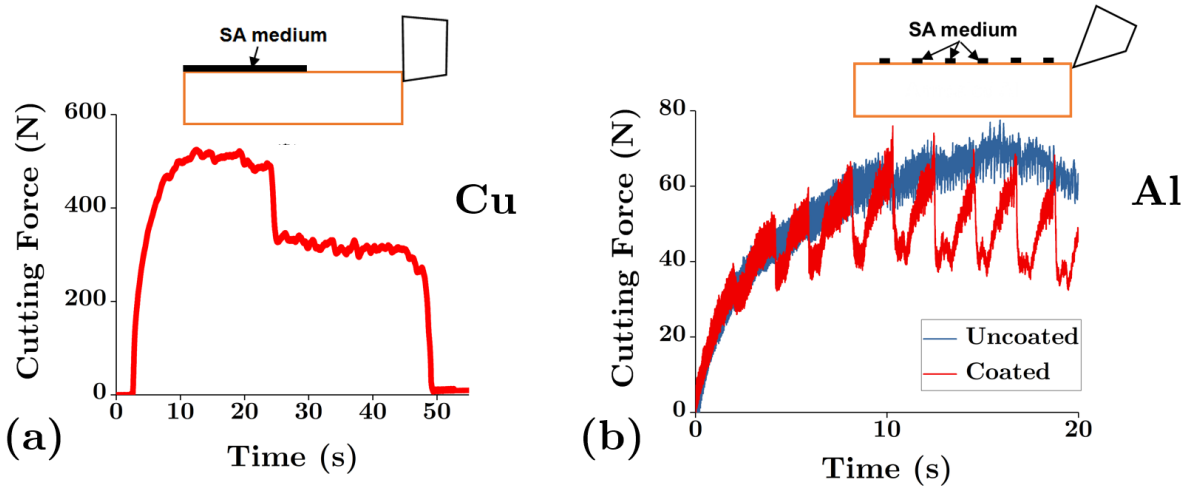

FIG. 6: Cutting forces reflect mechanochemical effects due to SA media. Forces for samples coated with SA media along half the cutting length (a) and in a periodic spot pattern (b). The latter force oscillates at a frequency matching the spot spacing. Note that the cutting force is the force component in the direction of the velocity.

specific energy. Furthermore, the energy reduction reflects the reduced strains accompanying segmented flow in the presence of SA media.

C. Flow perturbation due to localized media application

To further demonstrate the mechanochemical effect of SA media, two other sets of experiments were carried out shown in **Fig. 6**. In the first, the initial half-length of the workpiece (Cu) was kept uncoated, thereby presenting fresh annealed material to the cutting tool; and the SA medium (ink 1) applied only to the latter half of the workpiece length, see inset to **Fig. 6a**. All other experimental conditions were unchanged. As expected, when cutting the uncoated/bare region, the forces were quite high ($F_B = 500N$) and a sharp reduction occurred when the tool traversed the coated region of the workpiece. In the second demonstration, periodically spaced spots of an SA medium (ink 1) were placed on the workpiece (annealed Al) surface along the sample length, see inset to **Fig. 6b**. The resulting force then oscillated between a high F_B and a low F_C, the oscillation frequency matching the spatial frequency of the spot pattern. These observations were quite repeatable with all the media that demonstrated significant mechanochemical effects.

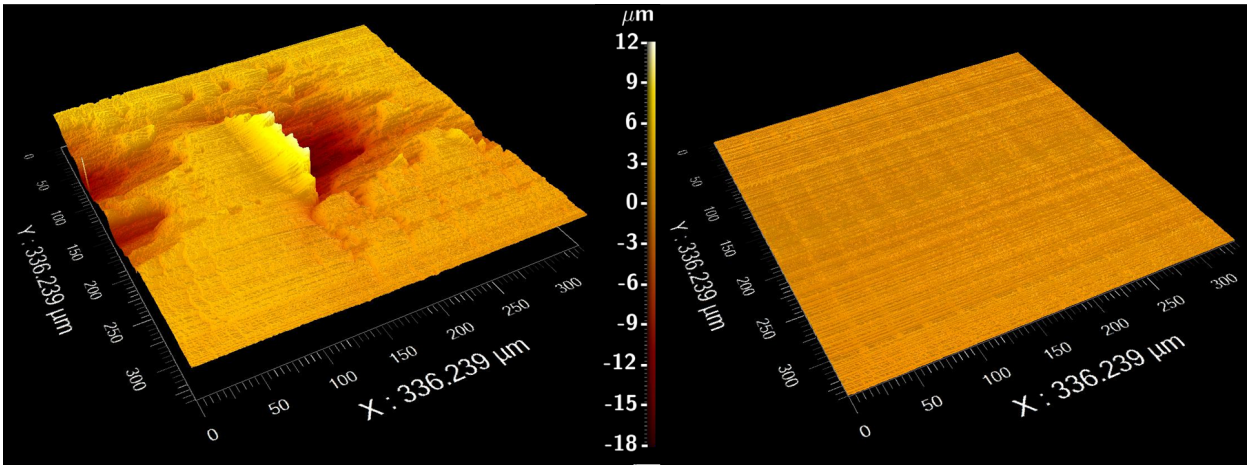

FIG. 7: 3-D surface profiles showing quality of the workpiece surface after cutting. (a) With sinuous flow, surface defects such as large pits (shown here) are very commonly observed. (b) With an SA media, the transition to segmentation-type flow results in an order of magnitude improvement in surface quality and finish, as measured by average pit size, pit density and surface roughness (R_a).

D. Surface defects and topography

Alongside transition in flow mode and attendant force reduction, the SA medium application was found to result in a remarkable improvement in quality of the newly created (cut) workpiece surface. As has been demonstrated clearly elsewhere, the occurrence of folding and sinuous flow is synonymous with the formation of pits, cracks and tears on the resulting surface [28, 33]. **Figure 7(a)** shows a 3D surface profile of a typical pit on the newly generated Cu surface arising from the folding process. The ratio of pit size (maximum depth from free surface) to initial tool penetration depth was $\Delta_P/h_0 \sim 0.75$, and the average pit area and density were 3.3×10^4 μm^2, 6.2 /mm^2 respectively, reflecting significant degradation of the newly formed surface. In the presence of the SA medium, where the folding process is interrupted by segmentation with much smaller forces, the resulting surface shows no pit/crack defects, see **Fig. 7b**. In fact, this drastic change in surface quality could also be ascertained by directly viewing the cut surface without any optical aids. Furthermore, the surface finish improved by an order of magnitude—R_a for annealed Cu $\alpha = 0^\circ$ was 4.4 μm without media and 0.55 μm with glue 1.

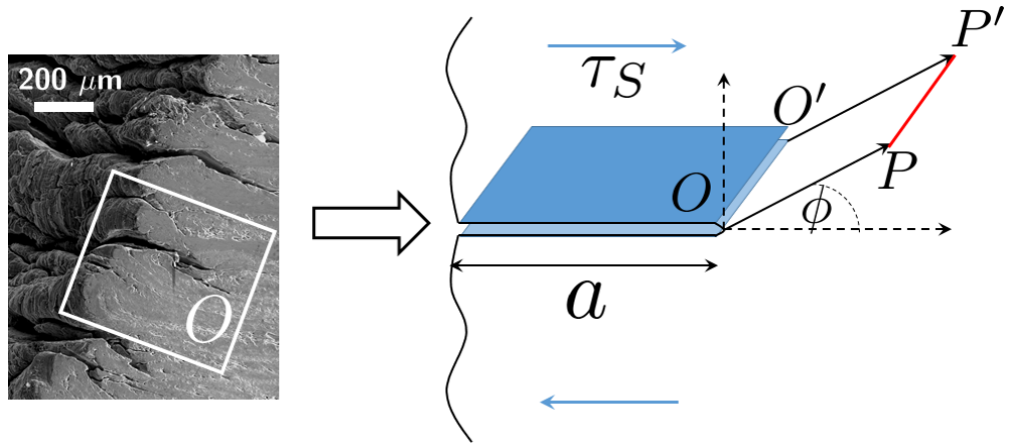

FIG. 8: Schematic of the model showing a fold pinning point (O) coinciding with the tip of a notch of length a, and causing increased local stress concentration under remote shear loading τ_S. Continued plastic deformation is enabled by emission of a dislocation (PP') from the tip OO' along a grain boundary oriented in the direction ϕ.

E. Analytical model: Mechanochemical effect as a local ductile-to-brittle transition

The observed mechanochemical effects of common SA media in metal cutting exhibit the three key characteristics that facilitate a ductile-to-brittle transition [34]—significant plastic deformation prior to fracture, crack nucleation during deformation and a mechanism for surface energy reduction. Based on the observations, these are caused by fold initiation, notch formation at pinning points and the applied SA medium, respectively. Each pinning point bounding a fold acts like a local stress concentrator or notch tip, see schematic in **Fig. 8**. In forming the chip, the tool imposes a remote shear τ_S on the workpiece. Within this framework, the transition from sinuous to segmentation-type flow corresponds to a competition between continued plastic deformation and unstable crack growth from O, respectively, in the presence of the SA medium. Quantitatively, this may be analyzed by considering the energetics of deformation at the tip O [35, 36].

For the geometry and loading in **Fig. 8**, the elastic stress field at the tip of the notch is [37]:

$$\sigma_{\rho\phi} = \frac{K_{II}}{2\sqrt{8\pi\rho}}\left[3\cos\frac{3\phi}{2} + \cos\frac{\phi}{2}\right] \qquad K_{II} = \zeta\,\tau_S\sqrt{a} \tag{1}$$

Where ζ is a dimensionless constant that depends on the precise shape of the free surface on either side of the notch tip O. The applied shear τ_S increases continuously from the onset

of plastic buckling and formation of the pinning point until it reaches a critical value τ_S^* for a crack of size a to grow from O, given by the Griffith criterion [38]

$$K_{II}^* = \zeta\, \tau_S^* \sqrt{a} = \sqrt{\frac{2E\gamma}{1-\nu^2}} \tag{2}$$

where E, ν are the Young's modulus and Poisson's ratio, respectively, and γ is the surface energy. An adsorbed SA medium alters the surface properties, viz. γ in Eq. 2.

As opposed to crack growth at $\tau_S = \tau_S^*$, the metal may continue to deform plastically in the vicinity of O by continuous dislocation emission and crack blunting [35].The net force acting on the dislocation shown in **Fig. 8** may be divided into 3 primary contributions: the force F_τ due to the applied remote shear loading τ_S, an image force F_I due to traction-free boundary conditions on the crack surfaces, and a ledge force F_L due to the formation of the dislocation from the crack edge O [39].

The force F_τ may be evaluated using the expression $\vec{F}_{PK} = (\sigma \cdot \vec{b}) \times \hat{t}$ as

$$\vec{F}_{PK} = \sigma_{\rho\phi} b_E = \left[\frac{E\gamma b}{4\pi(1-\nu^2)}\right]^{\frac{1}{2}} \frac{f(\phi)}{\sqrt{\xi}}\, \cos\psi\, \hat{\rho} \tag{3}$$

here $\hat{t}$, $\vec{b}$ represent the dislocation line direction and Burgers' vector, respectively and ψ is the angle between them. The constants E, γ, ν are the Young's modulus, surface energy and Poisson's ratio, respectively. ξ is the dimensionless radius coordinate $\xi = \rho/b$. It is implicitly assumed in this expression that the remote shear stress τ_S is equal to the critical stress for crack growth. The function $f(\phi)$ is the material-independent expression for the angular dependence of the stress $\sigma_{\rho\phi}$

$$f(\phi) = \frac{1}{2}\left[3\cos\frac{3\phi}{2} + \cos\frac{\phi}{2}\right] \tag{4}$$

The image force on the dislocation may be computed directly using thermodynamic arguments [39] as:

$$F_I = \vec{F}_i = -\frac{Eb(1-\nu\sin^2\psi)}{8\pi(1-\nu^2)}\,\frac{1}{\xi}\,\hat{\rho} \tag{5}$$

Similarly, using the Peierls model of a dislocation with core radius ξ_C, the ledge force is approximated as [37]

$$F_L = -\frac{2}{\pi}\frac{\gamma\alpha\cos\psi\sin\phi}{\xi^2+\alpha^2} \qquad \alpha = e^{3/2}\frac{\xi_C}{2} \tag{6}$$

This force, F_L, is negligible when compared to F_I, F_τ so that a good approximation for the equilibrium distance ξ^* is obtained by evaluating $F = F_I + F_\tau = 0$. The equilibrium distance ρ^* at which the two forces are balanced is then given by:

$$\begin{aligned} \xi^* = \frac{\rho^*}{b} &= \frac{(1-\nu\sin^2\psi)^2}{8\pi(1-\nu)}\,\frac{\mu b}{\gamma}\left(\frac{1}{f(\phi)\cos\psi}\right)^2 \\ f(\phi) &= \frac{1}{2}\left[3\cos\frac{3\phi}{2} + \cos\frac{\phi}{2}\right] \end{aligned} \tag{7}$$

where $\mu = 2E/(1+\nu)$ is the shear modulus. This expression for ξ^* is determined purely by the notch geometry and material properties, and not by the loading τ_S. For a given configuration, the ability of the crack tip to emit dislocations along a certain direction ϕ, causing further plastic deformation without crack growth, is obtained by ξ^* and the dislocation core radius ξ_C: If $\xi^*/\xi_C > 1$, then any dislocation emitted at O must overcome an energy barrier to reach equilibrium at ξ^* and blunt the crack. In this case, crack growth from O is more favorable and segmentation-type flow ensues. On the other hand, if $\xi^*/\xi_C < 1$, then dislocation emission is favorable so that the crack tip is blunted and the stress concentration lowered. Now $K_{II} < K^*_{II}$ and the crack does not grow from the pinning point O. Note that since pinning points coincide with ends of grain boundaries, and since dislocations are most easily emitted along these boundaries, ϕ approximately denotes grain boundary orientation.

The flow in the presence of SA medium is easily predicted by comparing curves for $\xi^*(\phi)$ from Eq. 7 for different metal-media combinations. This is shown for bare/uncoated annealed Cu (black curve, surface energy $\gamma = \gamma_0$, $\mu b/\gamma_0 = 6.1$ [35]) in **Fig. 9**. An SA medium changes γ, depending on the strength of the metal-medium interface, resulting in a different $\xi^*(\phi)$ curve, see plots for $\gamma = 0.5\gamma_0, 0.2\gamma_0, 0.1\gamma_0$ are also shown in red, blue, green, respectively. It is clear that for an order of magnitude change in γ, the $\xi^*(\phi)$ curve now almost entirely lies above the $\xi^*/\xi_C = 1$ line (dashed) so that crack growth along nearly all grain boundary orientations is more favorable compared to continued plastic deformation. Thus, almost every pinning point should lead to segment formation (*cf.* **Fig. 2 bottom row**) in the presence of a strongly adhering SA medium. We have obtained a preliminary lower-bound estimates for $\gamma/\gamma_0 \approx 0.7$ from molecular dynamics simulations for weakly adsorbed systems that demonstrated no mechanochemical effects (see appendix). Based on the experimental observations, it appears reasonable to expect $\gamma/\gamma_0 < 0.1$ for strongly adsorbing media such as glues and marking inks. Therefore, even with this conservative estimate of $\gamma = 0.2\gamma_0$ with

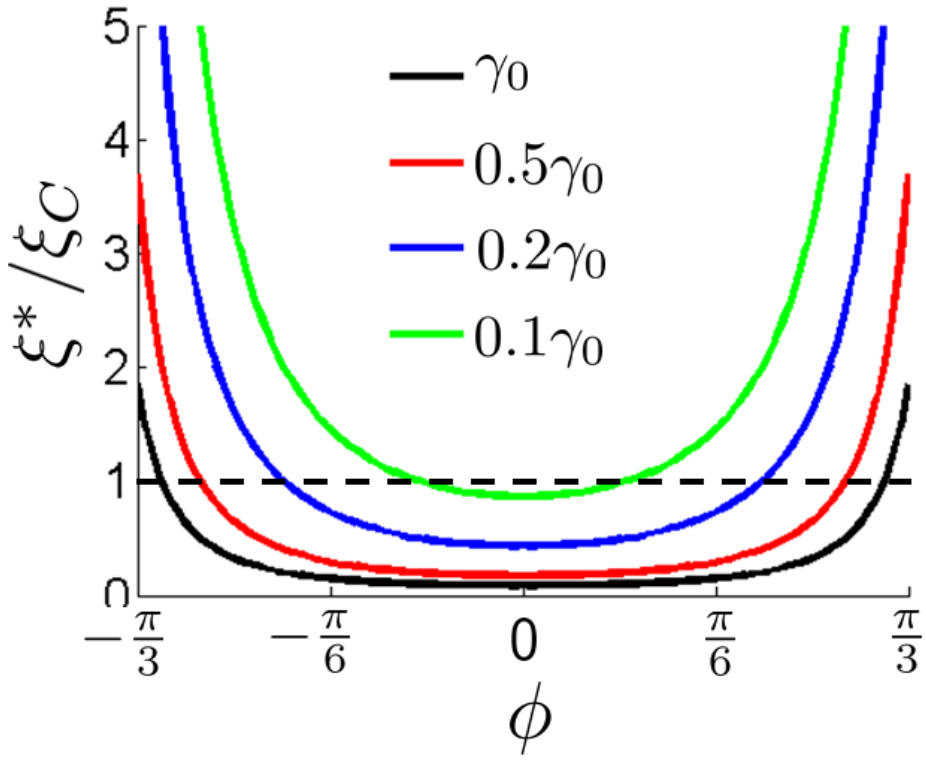

FIG. 9: Equilibrium dislocation distance ξ^*/ξ_C as a function of grain boundary orientation for varying surface energy γ. An order of magnitude change, from the uncoated metal (γ_0) to one with a suitable SA medium ($0.1\gamma_0$) favors crack growth as opposed to plastic deformation for nearly all grain boundary orientations. This corresponds to a complete local transition from sinuous to segmentation-type flow, giving rise to the mechanochemical efect. Data is for Cu with $\mu b/\gamma_0 = 6.1$

SA media, the model predicts that it is favorable for crack growth to occur along directions $\phi > \pi/6$ (blue curve, **Fig. 9**).

IV. DISCUSSION

The observations have shown that a variety of chemical media, which adsorb strongly (physically) onto surfaces, cause significant reductions in the forces and energy when cutting soft metals, as highlighted by the results from cutting of Cu, Al and Fe in an initially annealed condition (**Figs. 4** and **5**). This force and energy reduction can be taken as one key signature of the mechanochemical effect. It should be noted that while the term "mechanochemical"

has been used to stay consistent with the literature [21], the interactions between the SA medium and the metal considered here mostly pertain to physisorption. The force and energy reductions are greatest with media that have the strongest adhesive interactions. For example, Group I media, which show strong adsorption with all three metals, cause force reductions typically of around 50% with all of the metals. This reduction is even greater with Group II media which are known for strong adhesive interactions with Al alone; here the force reduction is as high as 80% with Al. However, the Group II media had only negligible influence on the force with annealed Cu and Fe, consistent with their known propensity to not adhere strongly to these metal surfaces. The results from Group III media further confirmed this hypothesis, that absent a strong adsorptive interaction with the metal surface, there is negligible impact on the forces. It may be recalled that Group III media are characterized only by a weak interaction with all of the three metals. The force reductions observed with the Group I and II media are also much greater than those reported in the past with CCL_4 as the chemical medium in cutting [18–20]. The results thus show that strong adsorptive interaction of the medium with the metal surface is a necessary condition for the mechanochemical effect to be manifest in cutting of metals.

Our experimental results have also shown that in addition to the strong adsorptive interaction between the media and the metal, a second condition is critical for the mechanochemical effect to occur. This condition is the need for sinuous flow, an unsteady flow mode, to prevail in the deformation zone. As seen from **Fig. 2**, this flow is characterized by large-amplitude material folding besides large strains. When the sinuous flow is much reduced or suppressed by changing the deformation geometry to $\alpha = 45^\circ$ (from $\alpha = 0^\circ$), or by pre-hardening the workpiece (H14 Al), the extent of the force reduction is significantly smaller or absent altogether, see **Fig. 5**. Under these conditions, smooth laminar (steady) flow becomes prevalent. The mechanochemical effect is now much smaller, indeed in most cases negligible, pointing to a strong coupling of the media action to the flow type.

The mechanism responsible for the major reduction in the forces with SA media is a transition in the deformation mode from sinuous flow, with material folding and excessive deformation, to a flow characterized by periodic fracture initiating from the metal surface the segmentation-type flow. This transition in the flow very much resembling a local ductile-to-brittle transition - has been directly captured by the *in situ* imaging, and also predicted by a simple model of the deformation that incorporates key flow attributes (e.g., notch-

like features) and the energetics of the SA medium-metal interaction. The mere presence of the SA medium on the surface induces the metal to behave in a brittle manner during the deformation, when sinuous flow prevails as with the annealed metals. The reason for this appears to be that sinuous flow produces stress-concentration features, locally, in the deformation zone that trigger local brittle behavior of the metal when the SA medium is present. As seen from the experimental observations, sinuous flow leads to the formation of mushroom shaped features at the surface due to the folding (see **Fig. 2a**). Interestingly, such folding has been reported to occur even at a nanometer length scale when cutting metals [40]. The pinning points between the folds are locations of high stress due to the notch-like geometry (see **Fig. 8**). In addition, the SA medium acts to decrease the surface energy of the metal by adhering to it. The combination of the notched geometry and lowered surface energy allow for a crack to propagate from the notch tip, leading to a segmentation-type flow mode.

As shown in Sec. IIIE, the presence of the SA medium at the tip of the notch embrittles the metal locally and allows for a crack to begin to propagate. Naturally, the question arises whether the SA medium is always in contact with the crack-tip, as it propagates from the free surface towards the tool tip. While it has not been possible to track the penetration of the SA medium into the cracks during segment formation, the following scenario appears to be the most likely. The SA medium embrittles the material in the vicinity of the notch, making crack-initiation at the free surface favorable. Once a crack-nucleates at the tip, it propagates naturally due to the dynamics of the loading, even through the tip itself might not subsequently contain the SA medium.

Per this crack-initiation mechanism, in the absence of crack nucleation sites, such as pinning points on the surface, mechanochemical effects should not be observed. This is again consistent with the experimental observations. When laminar flow is the dominant deformation mode, then since the folding is absent, there are no notch-like stress concentration features developing on the metal surface. Then the surface energy reduction effected by the SA medium is likely not sufficient to cause the laminar flow to transition to a segmentation-type flow. Under these conditions, a noticeable force reduction is not observed with the SA media, see results for hardened Al (H14) and $\alpha = 0^\circ$ for annealed Cu and Al (**Fig. 5**). In fact, similar behavior with regard to presence of defect features on the initial surface has also been observed in the case of liquid metal embrittlement [16]. It is thus suggested that the

action of the SA medium is to effect a local ductile-to-brittle transition. The beneficial consequences of ensuing flow transition are significant—smaller forces, energies and strains in surface generation, and an order of magnitude improvement in surface quality as measured by surface topography and defect density.

We have seen the mechanochemical effect to prevail when the sinuous flow occurs, because this type of unsteady flow provides the impetus for fracture instabilities to occur via crack nucleation at suitable surface pinning points. This raises a broader scientific question as to whether similar flow/fracture transitions, with beneficial effects, can be effected with other unsteady deformation modes like shear banding. Such modes are not infrequently observed in deformation processing and include analogous pinning points. This question is currently under study.

The mechanochemical effect described in this study is somewhat unique in that it is not material-specific. Since the effect is observed not only with glues of different chemical compositions (*cf.* Glues 1,2 and 3), but also with other media such as inks, it points to the fact that the bonds that form between the medium and the metal cannot be material-specific but arise due to electrostatic interactions. It is well-known that bonds that form between glues and metal surfaces, mediated by van der Waals force, are precisely of this nature [30].

Given that glues and inks adhere to nearly all metals, the beneficial effects of surface-active media demonstrated herein should open up new opportunities in cutting, stamping, piercing and forming of soft and highly strain-hardening metals like Fe, Al, Ta, stainless steels and Ni alloys. These metals are well-known as being just as difficult to process as hard metals, though because of their softness. The benign nature of the surface active media—in fact most of these are commonly used in everyday life and household practice–also means that this effect can be easily implemented in industrial settings.

V. CONCLUSIONS

A mechanochemical effect in cutting and large-strain deformation of metals is demonstrated using high-speed, *in situ* imaging of deformation and flow, complemented by force measurements. In cutting of soft metals and highly strain-hardening metals like aluminum, copper and iron, this effect is characterized by reduction in cutting forces and energy by up to 80% when a suitable chemical surface-active medium is merely coated onto the metal

surface prior to the cutting. The key conditions for the effect to be manifest are a) strong physical adsorption (adhesion) of the medium to the metal surface and b) occurrence of an unsteady plastic flow mode sinuous flow characterized by large-amplitude folding and large strains. This mechanochemical effect is distinguished from other catastrophic mechanochemical effects such as liquid metal embrittlement and stress corrosion cracking in that it is controllable, not material specific and effected by common household media like glues and inks. Another unique feature is coupling of the media action to the flow mode. The mechanism underlying the effect and force reduction is a transition in the deformation mode - from sinuous flow, which commonly prevails in the cutting of these highly strain-hardening metals, to a segmentation-type flow in the presence of the chemical medium. Direct observations and modeling show this flow transition to occur via a local change in the behavior of the metal surface from ductile to brittle, which arises from a lowering of the surface energy of the metal and formation of notch-like features due to the folding from the sinuous flow. Concomitant with the flow transition and force reduction, an order of magnitude improvement in the quality of the cut surface has been observed. The benign nature and simplicity of the media with which these beneficial effects are observed suggests interesting possibilities for enhancing performance of cutting and forming processes for metal alloys.

ACKNOWLEDGEMENTS

The authors would like to acknowledge support from US Army Research Office Award W911NF-15-1-0591, NSF grants CMMI 1562470 and DMR 1610094, and the US Department of Energy EERE program via Award DE-EE0007868.

---

[1] J. E. Williams, E. F. Smart, and D. R. Milner, Metallurgy of machining. Part 1: Basic considerations and the cutting of pure metals, Metallurgia **81**, 3 (1970).

[2] H. Yeung, K. Viswanathan, W. D. Compton, and S. Chandrasekar, Sinuous flow in metals, P. Natl. Acad. Sci. USA **112**, 9828 (2015).

[3] G. Schneider, Machinability of metals, American Machinist (2009).

[4] K. Viswanathan, A. Udupa, H. Yeung, D. Sagapuram, J. B. Mann, M. Saei, and S. Chandrasekar, On the stability of plastic flow in cutting of metals, CIRP Annals-Manufacturing

Technology **66**, 69 (2017).

[5] A. Udupa, K. Viswanathan, Y. Ho, and S. Chandrasekar, The cutting of metals via plastic buckling, Proc. R. Soc. A **473**, 20160863 (2017).

[6] H. Yeung, K. Viswanathan, A. Udupa, A. Mahato, and S. Chandrasekar, Sinuous flow in cutting of metals, Phys. Rev. Appl. **8**, 054044 (2017).

[7] Pliny, *Natural History* (1847) translated by Philemon Holland.

[8] K. H. Brown, D. A. Grose, R. C. Lange, T. H. Ning, and P. A. Totta, Advancing the state of the art in high-performance logic and array technology, IBM J. Res. Dev. **36**, 821 (1992).

[9] M. Krishnan, J. W. Nalaskowski, and L. M. Cook, Chemical mechanical planarization: slurry chemistry, materials, and mechanisms, Chem. Rev. **110**, 178 (2009).

[10] A. R. C. Westwood, N. M. Macmillan, and R. S. Kalyoncu, Chemomechanical phenomena in hard rock drilling, Int. J. Rock Mech. Min. Sci. **11**, A233 (1974).

[11] A. R. C. Westwood and J. J. Mills, in *Surface Effects in Crystal Plasticity*, edited by R. M. Latanision and J. T. Fourie (Nordhoff, Leyden, 1977) see also discussion by A. Argon, following the article.

[12] O. Reynolds, Chem. news 29, 117-118 (1874); mem, Proceedings of the Literary and Philosophical Society of Manchester **13**, 93 (1874).

[13] W. D. Robertson, *Stress Corrosion Cracking and Embrittlement* (J. Wiley, 1956).

[14] W. Rostoker, J. McCaughey, and H. Markus, *Embrittlement by Liquid Metals* (Reinhold Pub. Corp., 1960).

[15] A. Westwood and M. Kamdar, Concerning liquid metal embrittlement, particularly of zinc monocrystals by mercury, Philos. Mag. **8**, 787 (1963).

[16] P. Fernandes and D. Jones, Specificity in liquid metal induced embrittlement, Eng. Fail. Anal. **3**, 299 (1996).

[17] P. Rehbinder, New physico-chemical phenomena in the deformation and mechanical treatment of solids, Nature **159**, 866 (1947).

[18] E. Usui, A. Gujral, and M. C. Shaw, An experimental study of the action of CCl_4 in cutting and other processes involving plastic flow, International Journal of Machine Tool Design and Research **1**, 187 (1961).

[19] E. M. Kohn, Role of extreme pressure lubricants in boundary lubrication and in metal cutting, Nature **197**, 895 (1963).

[20] P. L. Barlow, Rehbinder effect in lubricated metal cutting, Nature **211**, 1076 (1966).

[21] P. A. Rehbinder and E. D. Shchukin, Surface phenomena in solids during deformation and fracture processes, Prog. Surf. Sci. **3**, 97 (1972).

[22] E. D. Shchukin, The influence of surface-active media on the mechanical properties of materials, Adv. Colloid Interface Sci. **123**, 33 (2006).

[23] J. R. Rice, in *Chemistry and Physics of Fracture*, edited by R. M. Latanision and R. H. Jones (1987) pp. 23–44.

[24] R. M. Latanision, in *Surface Effects in Crystal Plasticity*, edited by R. M. Latanision and J. T. Fourie (Nordhoff, Leyden, 1977).

[25] C. Cassin and G. Boothroyd, Lubricating action of cutting fluids, Journal of Mechanical Engineering Science **7**, 67 (1965).

[26] K. Nakayama, in *Proceedings of International Conference on Production Engineering* (1974) pp. 572–577.

[27] By the same token, some surfactants may also be termed surface-active. We use the term surface-active (SA) throughout the manuscript.

[28] K. Viswanathan, A. Mahato, H. Yeung, and S. Chandrasekar, Surface phenomena revealed by in situ imaging: studies from adhesion, wear and cutting, Surf. Topogr. Metrol. Prop. **5**, 014002 (2017).

[29] G. Gottstein, A. King, and L. Shvindlerman, The effect of triple-junction drag on grain growth, Acta Mater. **48**, 397 (2000).

[30] E. M. Petrie, *Handbook of Adhesives and Sealants (McGraw-Hill Handbooks)* (McGraw-Hill Education, 2007).

[31] A. R. Anderson and W. E. Smith, Processes for preparing metal alkyls and alkoxides, US Patent 2,965,663 (1960).

[32] O. Helmboldt, L. Keith Hudson, C. Misra, K. Wefers, W. Heck, H. Stark, M. Danner, and N. Rsch, Aluminum compounds, inorganic, in *Ullmann's Encyclopedia of Industrial Chemistry* (Wiley-VCH Verlag GmbH & Co. KGaA, 2000).

[33] A. Mahato, Y. Guo, N. K. Sundaram, and S. Chandrasekar, Surface folding in metals: a mechanism for delamination wear in sliding, Proc. R. Soc. A **470**, 20140297 (2014).

[34] A. H. Cottrell, Theory of brittle fracture in steel and similar metals, T. Metall. Soc. AIME **212**, 192 (1958).

[35] J. R. Rice and R. Thomson, Ductile versus brittle behaviour of crystals, Philos. Mag. **29**, 73 (1974).

[36] B. Bilby, A. Cottrell, and K. Swinden, The spread of plastic yield from a notch, Proc. R. Soc. A **272**, 304 (1963).

[37] M. Williams, The bending stress distribution at the base of a stationary crack, J. Appl. Mech. **24**, 109 (1957).

[38] J. F. Knott, *Fundamentals of Fracture Mechanics* (Butterworths, London, 1973).

[39] J. Hirth and J. Lothe, *Theory of Dislocations* (McGraw-Hill, New York, 1968).

[40] N. Beckmann, P. Romero, D. Linsler, M. Dienwiebel, U. Stolz, M. Moseler, and P. Gumbsch, Origins of folding instabilities on polycrystalline metal surfaces, Phys. Rev. Appl **2**, 064004 (2014).

[41] S. Plimpton, Fast parallel algorithms for short-range molecular dynamics, J. Comput. Phys. **117**, 1 (1995).

[42] M. Aryanpour, A. C. van Duin, and J. D. Kubicki, Development of a reactive force field for iron- oxyhydroxide systems, J. Phys. Chem. A **114**, 6298 (2010).

[43] U. O. M. Vázquez, W. Shinoda, P. B. Moore, C.-c. Chiu, and S. O. Nielsen, Calculating the surface tension between a flat solid and a liquid: a theoretical and computer simulation study of three topologically different methods, J. Math. Chem. **45**, 161 (2009).

[44] T. L. Hill, *An introduction to statistical thermodynamics* (Addison-Wesley, Reading, 1960).

[45] S. Schönecker, X. Li, B. Johansson, S. K. Kwon, and L. Vitos, Thermal surface free energy and stress of Iron, Sci. Rep. **5**, 14860 (2015).

Appendix A: Atomistic simulations for surface energy estimates

Metal-media interactions were studied using molecular dynamics simulations, performed using the open-source software LAMMPS [41]. The specific aim of these simulations was to estimate the change in surface energy of the metal due to contact with a typical SA agent. Change in surface energy is related to the strength of bonds that develop between the metal and the media. In order to predict the formation of any potential bonds the ReaxFF potential was used [42]. Due to limited availability of data on potentials for SA media and metals, the surface energy calculations were done for the interaction between

isopropyl alcohol and pure Fe alone, for which potentials are available.

An orthorhombic box (7 nm $\times$ 7 nm $\times$ 3 nm) containing Fe atoms in a bcc lattice was created with a lattice parameter of 2.856 $\mathring{A}$. Periodic boundary conditions were imposed in the X and Y direction, while the box is bounded in the Z direction by free surfaces whose properties are to be studied. A timestep of 0.25 fs was used and the system temperature was maintained at 300 K using a Langevin thermostat. The system of Fe atoms was equilibrated (as indicated by the total energy) by running the simulation for 20000 timesteps. In a separate simulation isopropyl alcohol molecules were generated using the Avagadro software. They were then equilibrated by running the simulation in LAMMPS for 20000 timesteps and monitoring the energy of the system.

The surface energy was calculated using the virial stress method [43, 44].This approach calculates the change in the stress in a direction perpendicular to the interface, due to the surface tension forces. The surface (interface) energy was calculated using the following formula,

$$\gamma = \frac{L_z}{2}\left[P_{zz} - \left(\frac{P_{xx} + P_{yy}}{2}\right)\right] \tag{A1}$$

Here γ refers to the surface/interface energy, L_z to the length of the orthorhombic box in the Z-direction, P_{ii} to the ith component of the stress tensor.

The surface energy of pure Fe, computed using this procedure, was obtained to be 2.19 J/m^2, which is close to the value that is usually reported [45]. The estimate was verified to be independent of system size by obtaining similar results for a box of different dimensions (4.8 nm $\times$ 4.8 nm $\times$ 1.5 nm).

Next, IPA molecules were introduced into the orthorhombic cell containing the Fe atoms, so that they could interact with the surfaces normal to the Z direction. The Fe-IPA system was allowed to equilibrate (as determined by total system energy) by running the simulation for 20000 timesteps. Using Eq. A1 again, the value of interface energy between Fe and IPA was calculated to be 1.64 J/m^2. This represents a decrease in the surface energy by 28%. It is expected that with molecules that adsorb strongly to the Fe surface, such as glues, the drop will be much greater.